The mammalian twisted gastrulation gene functions in foregut and craniofacial development

Anna Petryk,[a,b] Ryan M. Anderson,[c] Michael P. Jarcho,[a] Irina Leaf,[b] Cathy S. Carlson,[d] John Klingensmith,[c] William Shawlot,[b] and Michael B. O'Connor[b,e,*]

[a] Department of Pediatrics, University of Minnesota, Minneapolis, MN 55455-0356, USA
[b] Department of Genetics, Cell Biology and Development, University of Minnesota, Minneapolis, MN 55455-0356, USA
[c] Department of Cell Biology, Duke University Medical Center, Durham, NC 27710-3709, USA
[d] Department of Veterinary Diagnostic Medicine, University of Minnesota, St. Paul, MN 55108, USA
[e] Howard Hughes Medical Institute, University of Minnesota, Minneapolis, MN 55455-0356, USA

Abstract

Extracellular modulators of cell–cell signaling control numerous aspects of organismal development. The Twisted gastrulation (Twsg1) gene product is a small, secreted cysteine-rich protein that has the unusual property of being able to either enhance or inhibit signaling by the bone morphogenetic protein (BMP) subfamily of TGF-β type factors in a context-dependent manner. In this report, we characterize the early embryonic and skeletal phenotypes associated with loss of Twsg1 function in mice. All *Twsg1* mutant mice, irrespective of genetic background, exhibit deletions of neural arches in the cervical vertebrae. In a C57BL/6 background, we also observe pronounced forebrain defects including rostral truncations, holoprosencephaly, cyclopia, as well as alterations in the first branchial arch (BA1) leading to lack of jaw (agnathia). Characterization of marker expression suggests that these defects are attributable to loss of signaling from forebrain-organizing centers including *Fgf8* from the anterior neural ridge (ANR) and *Shh* from the prechordal plate (PrCP). In addition, we find defects in the foregut endoderm and a reduction in *Hex* expression, which may contribute to both the forebrain and BA1 defects.
© 2003 Elsevier Inc. All rights reserved.

Keywords: Twisted gastrulation; Mouse; BMP; Holoprosencephaly; Forebrain; Neural arch; Agnathia; Foregut

Introduction

The vertebrate head is initially organized around two primordial structures, the anterior neural plate and the foregut endoderm. Recent work has demonstrated that the nascent foregut has a critical role in promoting forebrain development (Martinez Barbera et al., 2000; Withington et al., 2001). Increasing evidence suggests that the pharyngeal portion of the foregut also has a critical role in development of craniofacial structures, such as the mandible and maxilla (Couly et al., 2002; Piotrowski and Nusslein-Volhard, 2000). The prechordal plate (PrCP), the rostral extremity of the axial mesendoderm, promotes ventral forebrain development and the elaboration of midline facial structures

(Shimamura and Rubenstein, 1997). Anterior ectoderm also plays an early role in forebrain development, such that the anterior neural ridge (ANR) promotes the growth of the telencephalon (Rubenstein and Beachy, 1998).

These developmental tissue interactions are mediated largely by secreted molecules and intercellular signaling pathways. Two key molecules that regulate forebrain and craniofacial development are Sonic hedgehog (SHH) and Fibroblast growth factor 8 (FGF8). In mouse embryos lacking *Shh*, the PrCP is deficient in inductive activity; consequently, the ventral midline of the brain is lost, resulting in holoprosencephaly, along with corresponding deletions of the facial midline, resulting in cyclopia (Chiang et al., 1996). FGF8 appears to mediate ANR signaling to promote forebrain growth (Shimamura and Rubenstein, 1997); mouse embryos hypomorphic for *Fgf8* show variable rostral truncations (Meyers et al., 1998; Storm et al., 2003). Local retinoid signaling coordinates forebrain and facial morphogenesis by maintaining FGF8 and SHH (Schneider

* Corresponding author. Department of Genetics, Cell Biology and Development, University of Minnesota, 6-160 Jackson Hall, Church Street SE Minneapolis, MN 55455-0356. Fax: +1-612-625-5402.
E-mail address: moconnor@gene.med.umn.edu (M.B. O'Connor).

et al., 2001). In contrast, bone morphogenetic protein (BMP) activity inhibits expression of *Shh* in the PrCP and *Fgf8* in the ANR, thereby interfering with normal forebrain and craniofacial development (Anderson et al., 2002; Ohkubo et al., 2002). Genetic reduction of the levels of the BMP antagonists Chordin (Chrd) and Noggin (Nog) results in truncations and midline deletions of both the forebrain and facial structures, suggesting that BMP signaling must be tightly regulated in vivo for rostral development (Anderson et al., 2002; Bachiller et al., 2000).

Twisted gastrulation has recently been shown to affect BMP signaling in both invertebrate and vertebrate species (Chang et al., 2001; Oelgeschlager et al., 2000; Ross et al., 2001; Scott et al., 2001). In *Drosophila*, Decapentaplegic (Dpp) is closely related to vertebrate BMP2 and BMP4, and Short gastrulation (Sog) is homologous to vertebrate Chrd. In this system, Tsg and Sog synergistically inhibit Dpp signaling (Ross et al., 2001). Twsg1 (called Tsg in non-mammals) is evolutionarily conserved and functionally equivalent among species. Loss-of-function studies in both zebrafish and *Xenopus* suggest that Tsg acts to antagonize BMP signals in the vertebrate system (Blitz et al., 2003; Ross et al., 2001). In addition, overexpression of either *Drosophila* or zebrafish Tsg mRNA dorsalizes zebrafish embryos, consistent with its ability to reduce BMP signaling, and in *Xenopus*, coinjection of *Chrd* and *Tsg* mRNAs synergistically enhances secondary dorsal axis formation within a certain concentration range of both mRNAs (Ross et al., 2001). The mechanism of synergism involves formation of tripartite complexes among Tsg, Chrd, and BMPs, thereby preventing binding of BMPs to their receptors (Chang et al., 2001; Oelgeschlager et al., 2000; Ross et al., 2001; Scott et al., 2001). Paradoxically, Tsg can act as a BMP agonist in *Xenopus* at high Tsg/Chrd concentration ratios (Larrain et al., 2001; Ross et al., 2001; Oelgeschlager, 2003) in part by promoting degradation of Chrd (Oelgeschlager et al., 2003).

To understand the role of Twsg1 in mammalian embryonic development, we have used gene targeting to generate mice lacking Twsg1 activity. The interaction of Twsg1 with the BMP signaling pathway suggests that Twsg1 may play important roles in mammalian development, given that BMPs play tissue-specific roles in regulating cell proliferation, differentiation, apoptosis, morphogenesis, and pattern formation (Hogan, 1996). A previous study of *Twsg1* mutant mice reported that they exhibited dwarfism, with half dying approximately 1 month after birth (Nosaka et al., 2003). However, the mutation used in that work differs from the one we have produced here and was not tested in different genetic backgrounds. We found that the phenotypes of *Twsg1* deficiency are highly dependent on genetic background. Although we observed growth retardation and wasting in a mixed genetic background, when *Twsg1* mice were backcrossed to C57BL/6 mice for five generations, we observed severe craniofacial defects and perinatal lethality. The rostral deletions we observed are very similar to those resulting from reduced levels of BMP antagonists Chrd and

Nog (Anderson et al., 2002) and are not enhanced by heterozygosity for either Chrd or BMP4. Our results indicate that *Twsg1* is important for early foregut, forebrain, and craniofacial development, as well as for axial skeletogenesis.

Materials and methods

Generation of Twsg1-deficient mice

A *Twsg1* genomic clone was obtained by screening a mouse genomic DNA library using a 2170-bp mouse *Twsg1* cDNA probe (*Xho*I–*Not*I fragment) containing the entire 666-bp coding region (cDNA clone AW258143 was obtained from Research Genetics). A 16-kb *Not*I fragment from a positive phage was subcloned into Bluescript II KS+ plasmid. The targeting vector was prepared using pDZ157 plasmid (Raymond et al., 2000) and electroporated into AB1 ES cells. Homologous recombination in G418-resistant ES cell clones was confirmed by PCR analysis of the 5′ region and Southern blot analysis using a 0.9-kb *Xba*I–*Ase*I 3′ probe outside the homologous region. Six of 266 G418-resistant clones were correctly targeted on both the 5′ and 3′ ends. Of the two injected clones, one gave rise to chimeric mice that transmitted the mutation through the germline. Heterozygous mice carrying a conditional allele of *Twsg1* (*Twsg1*^neo/+^) were bred to *βactin-Cre* mice (Lewandoski et al., 1997) to remove exon 3. Mice heterozygous for deletion of exon 3 are called *Twsg1*^+/−^. Because the presence of the PGKneomycin (PGK*neo*) cassette may affect the phenotype of the mice, *Twsg1*^+/−^ mice were also bred to *βactin*-FLPe mice (Rodriguez et al., 2000) to remove the PGK*neo* cassette. Heterozygous mice lacking the PGK*neo* cassette were intercrossed to generate homozygotes.

Generation of double mutants

Twsg1^+/−^ mice in a mixed genetic background (129Sv/Ev, C57BL/6, and FVB/N) were bred to *Chrd*^+/−^ mice in a 129Sv/J background (Bachiller et al., 2000) and *Bmp4*^lacZ^ mice in an ICR background (Lawson et al., 1999) to generate double heterozygous progeny. Timed matings were set up to analyze compound mutants at various gestational stages.

Genotyping

Genomic DNA was isolated from tails or yolk sacs by standard methods (Hogan et al., 1994). *Twsg1* mice were genotyped by polymerase chain reaction (PCR parameters: 40 cycles, 94°C for 30 s, 60°C for 1 min, and 72°C for 5 min). Amplification of a wild-type (WT) allele generated a 2.9-kb product, and a 2-kb product in the case of a mutant allele using the following primers: P4: 5′-tgaggacagaggag-catgcg-3′, P5: 5′-ggaggggagtttggaacttg-3′, and NeoF: 5′-tggaaggattggagctacgg-3′. *Chrd* alleles were genotyped as previously described (Bachiller et al., 2000). *Bmp4*^lacZ^

alleles were identified by PCR analysis for *lacZ* sequences using the following primers: LacZ Forward, 5′-acccaact-taatcgccttgc-3′; and LacZ Reverse, 5′-aacaaacggcggattgacc-3′ (PCR parameters: 30 cycles, 94°C for 30 s, 55°C for 45 s, and 72°C for 55 s).

Northern blot analysis

Total RNA was isolated from adult mouse heart and kidney using TRI Reagent (Molecular Research Center). Northern blot analysis was performed as described (Petryk et al., 2000) using a ^{32}P-labeled 536-bp mouse Twsg1 cDNA probe containing part of the coding region (NheI–NcoI fragment).

In situ hybridization

Whole-mount RNA in situ hybridization was performed by standard methods (Hogan et al., 1994; Wilkinson and Nieto, 1993). The probes used have been previously described (Crossley and Martin, 1995; Echelard et al., 1993; Sasaki and Hogan, 1993; Tao and Lai, 1992; Thomas et al., 1998).

Skeletal preparation and histology

The skeletons of wild-type and *Twsg1*$^{-/-}$ embryos and neonates were stained with alizarin red and alcian blue as described (Hogan et al., 1994). For histology, animals were fixed in 4% paraformaldehyde or Bouin's fixative, washed in PBS, dehydrated through alcohols, embedded in paraffin wax, and sectioned at 7 μm according to standard protocols. The vertebrae from 3-week-old mice were fixed in 4% paraformaldehyde, washed in PBS, embedded in paraffin wax, serially sectioned at 7 μm, and stained with hematoxylin or eosin.

Results

Mice lacking Twsg1 are viable but exhibit multiple phenotypes in mixed genetic backgrounds

Twsg1 has previously been reported to be expressed in multiple tissues during gastrulation, neurulation, and organogenesis stages such as the neural plate, neural tube, somites, branchial arches, surface ectoderm, and endoderm (Graf et al., 2001). Given the widespread expression of *Twsg1*, we designed a gene ablation strategy that would allow for tissue-specific targeting, if necessary, to reveal the roles of *Twsg1* in particular contexts (Fig. 1A). We prepared a gene replacement vector where exon 3 is flanked by loxP sites thereby allowing for deletion of exon 3 upon exposure to Cre recombinase (Raymond et al., 2000). Exon 3 encodes part of the N-terminal domain of Twsg1 (amino acids 74–162), which has the BMP-binding activity (Oelgeschlager et al.,

2000). After germline transmission of a targeted ES cell line (*Twsg1*$^{neo/+}$), deletion of exon 3 was achieved by breeding *Twsg1*$^{neo/+}$ mice to transgenic mice that express Cre recombinase in all cells of the embryo (Lewandoski et al., 1997). The resulting *Twsg1*$^{+/-}$ mice, of a mixed genetic background (129Sv/Ev, C57BL/6, and FVB/N), were mated to each other to produce *Twsg1*$^{-/-}$ homozygotes, which were viable and fertile. Analysis of *Twsg1* transcript levels in adult tissues (heart, kidney, liver) from *Twsg1*$^{+/+}$, *Twsg1*$^{+/-}$, and *Twsg1*$^{-/-}$ mice revealed the presence of a truncated *Twsg1* message in mice carrying mutant allele(s) (Fig. 1E). Although *Twsg1* message persists in homozygotes, the allele generated is likely to be null for BMP binding based on molecular alterations of the locus.

These mixed-background *Twsg1*$^{-/-}$ mice were smaller than wild-type (WT) or heterozygous siblings, and had short, kinked tails. The difference in size was most noticeable at weaning (21 days) and persisted through adulthood (Fig. 2A). At 3 weeks, the weight of *Twsg1*$^{-/-}$ males and females was about 66–68% of that of WT mice, and at 12 weeks, the weight of the knockout mice was about 80% of that of WT mice. The most severely affected homozygous mice (the 4% with the lowest weight) did not survive the first week after weaning due to generalized wasting (Table 1). To test whether the presence of the PGK*neo* cassette affected the phenotype of *Twsg1*$^{-/-}$ mice, we removed the PGK*neo* cassette. We found that the phenotype of homozygous *Twsg1* mice without the PGK*neo* cassette was identical to the phenotype of *Twsg1*$^{-/-}$ mice.

The observation that *Twsg1*-deficient mice have kinky tails in addition to growth failure prompted us to examine the skeletons of the mutants. We observed a significant delay in the ossification of cervical and coccygeal vertebrae in newborns (Figs. 2B–E). In the cervical and upper thoracic regions, the neural arches (which enclose the spinal cord dorsally) were truncated or discontinuous (Figs. 2H–K). Several coccygeal vertebrae were missing, resulting in shortening of the tail. Histological examination confirmed lack of development of the laminae of the neural arches (Figs. 2L,M) with partial preservation of the spinous process (Figs. 2N,O) in some vertebrae. The spinous process had diminished marrow space and consisted of immature cartilage (Fig. 2O) as opposed to mature, ossified bone in WT vertebrae (Fig. 2N). Abnormal formation of the neural arches was evident as soon as ossification of the neural arches was noticeable at E16.5 (not shown) and persisted until adulthood (2F,G), potentially exposing the underlying spinal cord to trauma. At several weeks of age, about 2% of *Twsg1*$^{-/-}$ mice exhibited neurologic symptoms, including stiffness, unsteady gait, or partial paralysis, particularly involving the hindlimbs.

Background-dependent craniofacial defects in Twsg1 mutants

Twsg1-deficient mice were backcrossed to the inbred C57BL6/J and 129/SvEv backgrounds (five generations)
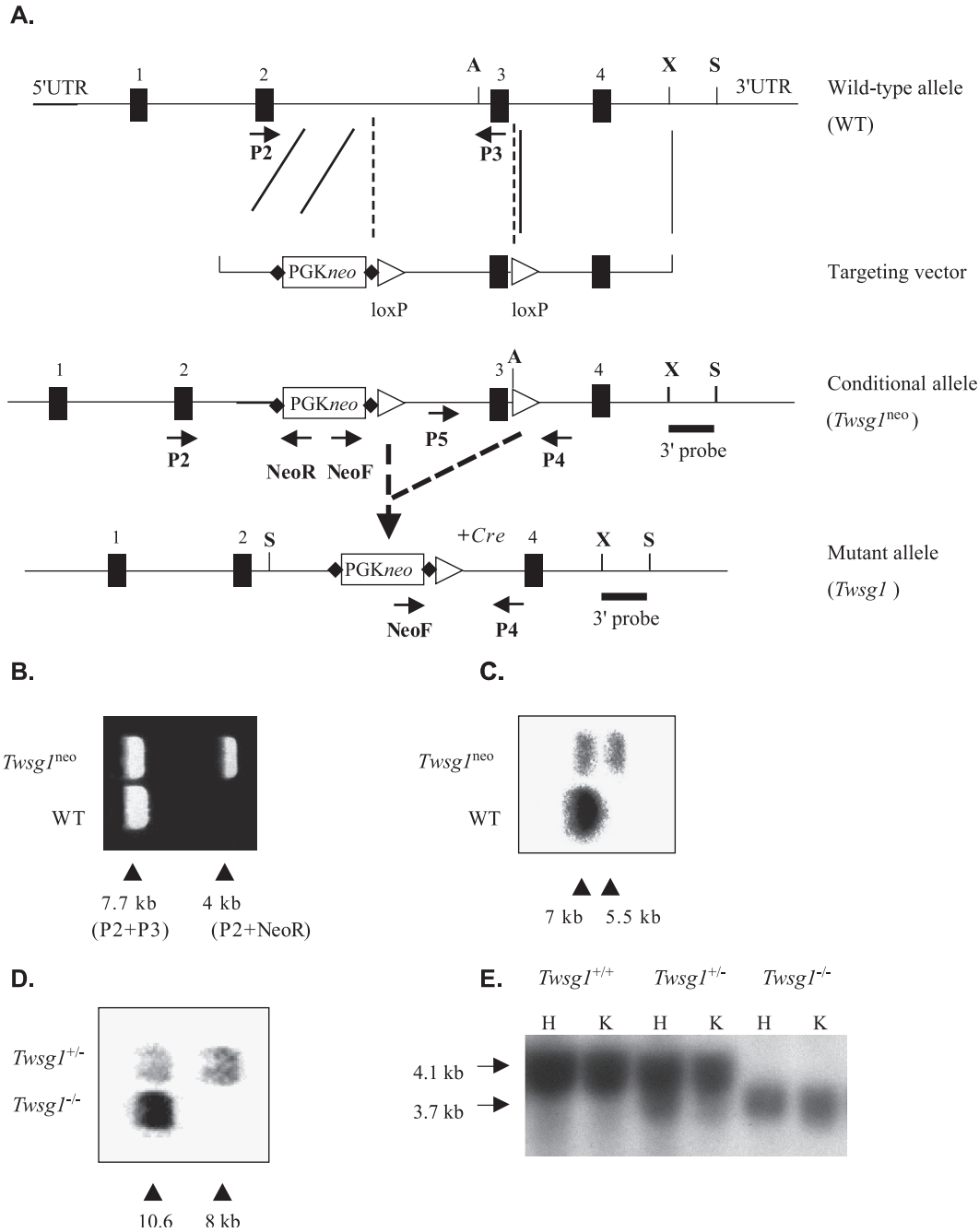
Fig. 1. The *Twsg1* gene targeting strategy. (A) The targeting vector contains a 2-kb 5′ homologous region, PGK*neo* cassette flanked by FRT sequences, followed by a 4.5-kb fragment flanked by loxP sites, and a 4.6-kb 3′ homologous region. An additional *Apa*I site was introduced on the 5′ end of the second loxP sequence to allow genotyping by Southern analysis. A, ApaI; S, AseI; X, XbaI. (B and C) Homologous recombination in ES cell clones was confirmed by PCR analysis of the 5′ region and Southern blot analysis using a 0.9-kb *Xba*I–*Ase*I 3′ probe outside of the homologous region. (B) Amplification with primers P2 (within exon 2) and P3 (within exon 3) produced a 7.7-kb fragment in wild-type alleles and amplification with primers P2 and NeoR (within the *neo* cassette) produced a 4-kb fragment in targeted alleles. (C) For Southern analysis, genomic DNA was digested with *Apa*I and *Ase*I and hybridized with a ^{32}P-labeled 3′ probe. The resultant fragments for wild-type alleles were 7 kb, and for targeted alleles 5.5 kb. (D) Southern analysis to confirm the removal of exon 3 by Cre recombinase. Genomic DNA was digested with *Ase*I and hybridized with a ^{32}P-labeled 3′ probe. The wild-type allele produced a 10.6-kb band, and the *Twsg1* allele without exon 3 produced an 8-kb band. (E) Analysis of *Twsg1* transcript levels in adult tissues (H, heart; K, kidney) from $Twsg1^{+/+}$, $Twsg1^{+/-}$, and $Twsg1^{-/-}$ mice revealed the presence of a truncated *Twsg1* message in mice carrying mutant allele(s).

to determine the effect of genetic background on *Twsg1* mutant phenotypes. Regardless of background, $Twsg1^{+/-}$ mice exhibit no visible abnormalities. The majority of $Twsg1^{-/-}$ mice in the 129/SvEv background were viable and fertile. The growth retardation was more pronounced than in mixed-background $Twsg1^{-/-}$ mice, and the frequency of lethality at birth (18%) and at weaning (12%) was increased (Table 1) for unknown reasons. At a gross level,
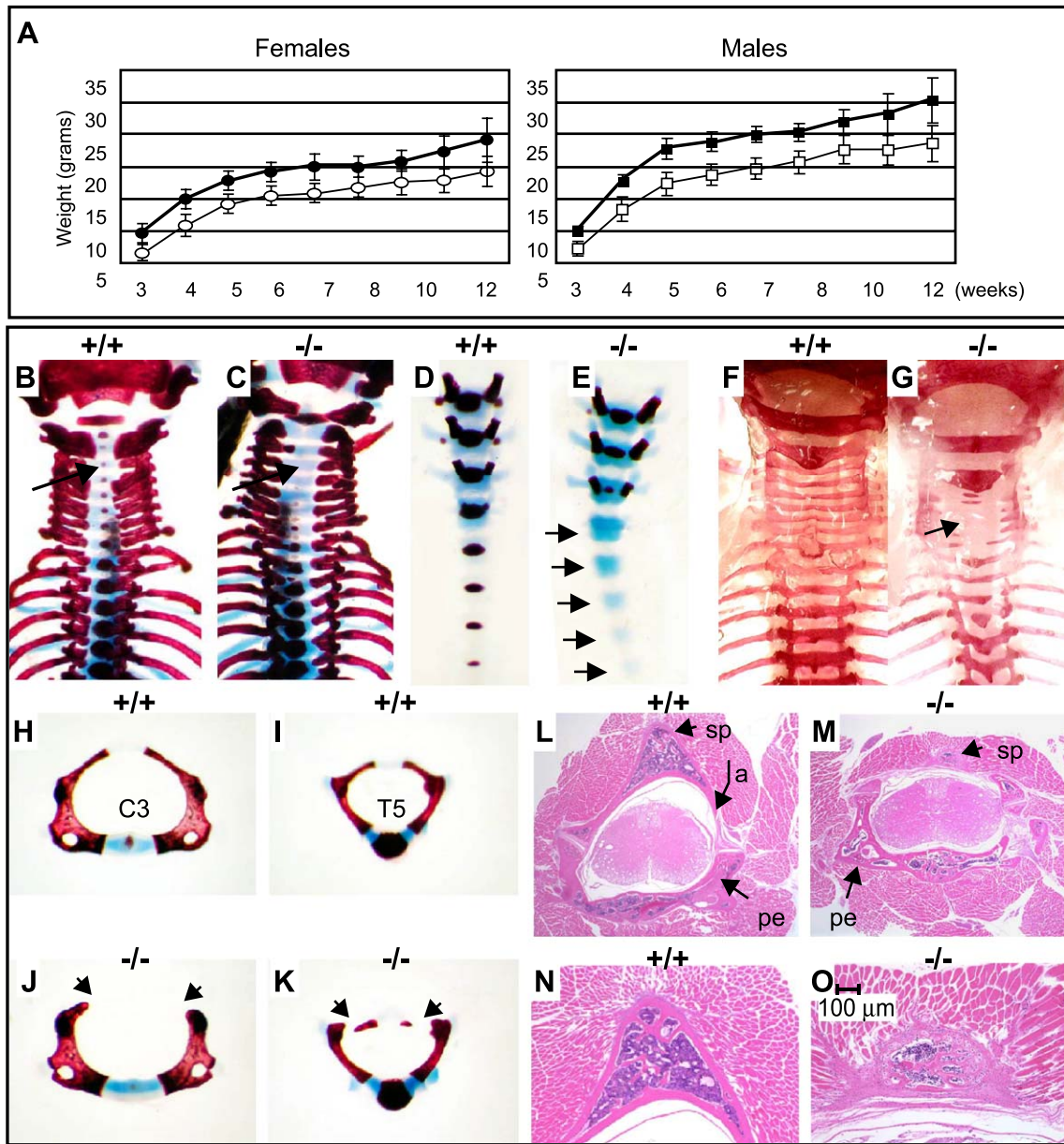
Fig. 2. (A) Postnatal growth failure in $Twsg1^{-/-}$ mice. (B–E) Skeletal preparations of wild-type and $Twsg1^{-/-}$ newborns. At birth, there is a significant delay in the ossification of cervical and coccygeal vertebrae. (F and G) Abnormal formation of the neural arches at 3 weeks of age. (H–K) Impaired development of neural arches in the cervical region (J) and upper thoracic (K) regions in $Twsg1$-deficient mice. (L–O) Histological examination of the cervical vertebrae of 3-week-old mice. (M) Lack of development of the laminae of the neural arches (la) with some preservation of the spinous process (sp) in $Twsg1$-deficient mice pedicle (pe). (O) The spinous process has diminished marrow space and immature cartilage. The specimens were serially sectioned to ensure that the level of the vertebra in each specimen was identical.

these $Twsg1$ homozygotes appeared to be morphologically normal; however, they too exhibited neural arch defects similar to those seen in the hybrid background (data not shown).

In the C57BL/6 background, $Twsg1^{-/-}$ mice suffer a high degree of perinatal lethality and craniofacial defects. The spectrum of craniofacial defects ranged from normal external appearance to very severe rostral truncations (Fig. 3). The rest of the body axis is essentially normal, and with the exception of the cervical vertebrae as noted above, the

defects are limited to rostral structures. To assess the frequency of specific craniofacial defects, we scored the phenotypes of 45 $Twsg1^{-/-}$ neonates in the C57BL/6 background. We found that only 18% of $Twsg1^{-/-}$ mice survived beyond the perinatal period (Table 1), while 38% of $Twsg1^{-/-}$ mice were perinatal lethal without gross morphological abnormalities, and the remaining 44% were perinatal lethal with various degrees of craniofacial defects. Out of 20 affected neonates, 10% had severe anterior truncation, with a loss of the rostralmost structures of the

Table 1
Mortality rates in $Twsg1^{-/-}$ mice in different genetic backgrounds

Age at death	$Twsg1^{-/-}$ 129/SvEv/C57BL/6/FVB/N ($N = 50$) (%)	$Twsg1^{-/-}$ 129/SvEv ($N = 19$) (%)	$Twsg1^{-/-}$ C57BL/6 ($N = 45$) (%)
Perinatal	0	16	82
>3 weeks of age	4	16	0

head (Fig. 3B). Another 70% had midline defects such as cyclopia or synophthalmia (partially fused eyes) with a proboscis, a long nasal process located above the eyefield (Fig. 3C), or single nostril with agnathia, that is, absence of the mandible (Fig. 3D). The remaining 20% had agnathia without other midline facial defects (Fig. 3E). The mice with single nostril or agnathia frequently exhibited defects in eye development ranging from microphthalmia to lack of eye development. The anatomical abnormalities were first noticeable at E9.0–E9.5. These phenotypes are similar to those observed in $Chrd^{-/-};Nog^{+/-}$ neonates (Anderson et al., 2002), though they occur at higher penetrance (44% vs. 9%). Although the craniofacial defects were most prevalent in C57BL/6 background, they were also observed in $Twsg1^{-/-}$ mice in 129/SvEv background (8th generation backcross). A significant number of these 129/SvEv mice (15%, 3/19) showed a moderate craniofacial defect that consisted of a reduced jaw phenotype.

Because midline facial defects may be indicative of brain defects, $Twsg1$-deficient mice were processed for histological examination. Transverse sections of WT and $Twsg1^{-/-}$

brains revealed defects typical of alobar holoprosencephaly (HPE), characterized by the failure of the prosencephalon to undergo median cleavage into bilateral cerebral hemispheres (Figs. 4A–D).

Activity of the Twsg1 protein modulates both Chrd function and BMP function, each of which has been previously implicated in forebrain development (Anderson et al., 2002; Bachiller et al., 2000; Furuta et al., 1997). To test whether the HPE phenotype of $Twsg1^{-/-}$ mice might be enhanced by a concomitant deficiency of either of these proteins, we generated double mutants in a mixed genetic background (129Sv/Ev, C57BL/6, FVB/N, 129Sv/J). $Twsg1^{-/-};Chrd^{+/-}$ mice were intercrossed and females sacrificed in late gestation (E15.5–E17.5). We did not find HPE phenotype in any of the 11 $Twsg1^{-/-};Chrd^{-/-}$ embryos from four matings. These embryos had the same phenotype as $Chrd^{-/-}$ embryos (Bachiller et al., 2003), including neural arch defects common to both $Chrd$ and $Twsg1$ mice. We also analyzed 13 $Twsg^{-/-};Bmp4^{+/-}$ embryos from 11 matings between E13.5 and E16.5 in a mixed background (129Sv/Ev, C57BL/6, FVB/N, ICR) and found none with external craniofacial defects. Because embryos homozygous for $Bmp4$ typically do not survive beyond E9.5 (Lawson et al., 1999), the predicted number of $Twsg1^{-/-};Bmp4^{+/-}$ embryos in late gestation would have been one in six. The observed number of embryos with $Twsg1^{-/-};Bmp4^{+/-}$ genotype was 13 out of 75, indicating that this genotype was not underrepresented later in gestation. Thus, we found no evidence for an enhancement of the $Twsg1$ craniofacial defects by reducing the BMP ligand gene $Bmp4$ or the BMP antagonist gene $Chrd$.
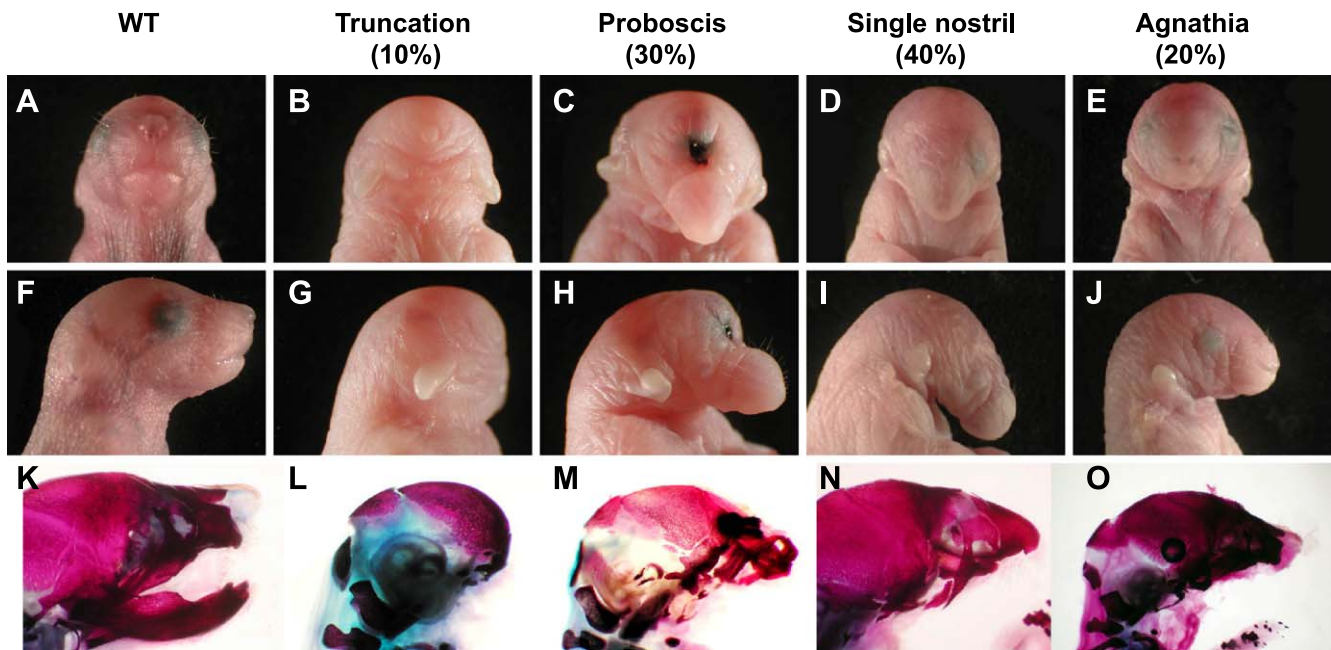

Fig. 3. The spectrum of rostral phenotypes in $Twsg1^{-/-}$ mice. (A) Wild type, (B) severe anterior truncation, (C) midline defects (cyclopia with proboscis), (D) single nostril with agnathia (absence of mandible), (E) agnathia alone. (F–J) Lateral view of newborn mice shown in A–E. (L–P) Skeletal preparations of animals shown in A–E.
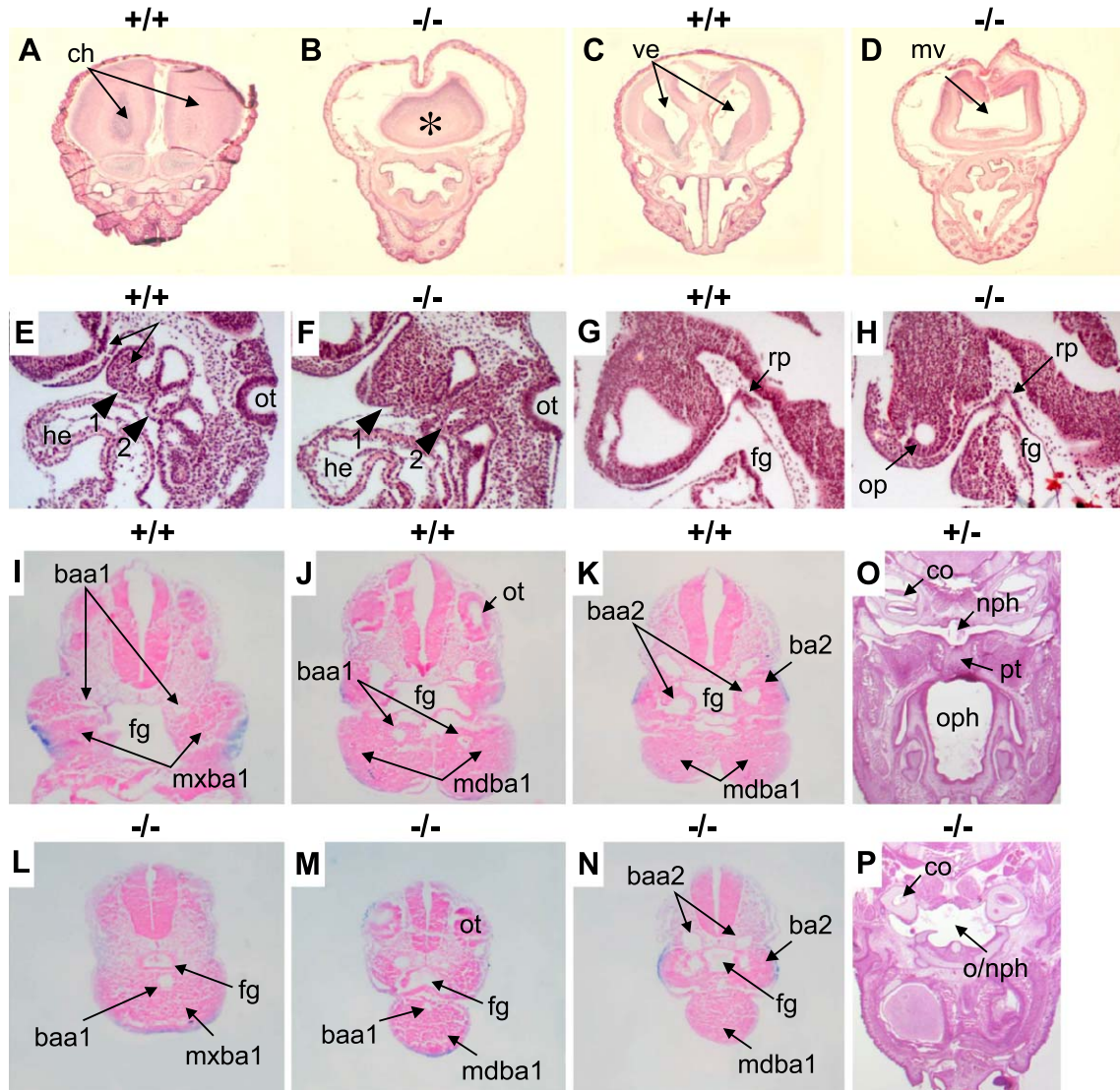
Fig. 4. (A–D) Transverse sections of wild-type and $Twsg1^{-/-}$ brains at birth. (A) Normal midline division of the cerebral hemispheres (ch) in wild-type mice. (B) Fused cerebral hemispheres in the mutants. (C) Symmetrical ventricular system (ve) in wild-type mice. (D) A large monoventricle (mv) in the mutants. (E) In WT embryos, bilateral first branchial arch (BA1) swellings segregate into maxillary and mandibular components indicated by the arrows; the arrow heads point to the first and second BA; he, heart; ot, otic vesicle. (F) Fused and enlarged BA1 in the mutants. (G and H) Small size of the foregut (fg) in the mutants as compared to wild-type mice; rp, Rathke's pouch; op, optic vesicle. (I and J) Separate maxillary (mxba1) and mandibular (mdba1) components of BA1 in normal mice containing two arteries (baa1). (K) Wild-type BA2 containing two arteries (baa2). (L and M) Fused BA1 in the mutants with a single artery. (N) Mutant BA2 containing two arteries (baa2). (O) Separation between the oropharynx (oph) and the nasopharynx (nph) by the palate (pt) in the wild-type mouse at birth. (P) Rudimentary oropharynx forming a common cavity with the nasopharynx; co, cochlea.

Abnormal first branchial arch in $Twsg1^{-/-}$ embryos

Deficient development of the lower jaw was observed in 60% of affected $Twsg1^{-/-}$ embryos in the C57BL/6 background. Because the mandible develops from the first branchial arch (BA1), we analyzed branchial arch development in E9.5 embryos. At that stage, BA1 is composed of four independent swellings formed by bilateral pairs of maxillary and mandibular prominences (Fig. 4E). This subdivision is absent in $Twsg1^{-/-}$ embryos, leading to the appearance of an enlarged BA1, fused at the ventral midline (Fig. 4F). In the WT embryos, BA1 also contains bilateral

aortic arch arteries (Figs. 4I,J), but in the mutant embryos there is only one BA1 artery (Figs. 4L,M). The second branchial arch appeared normal (Figs. 4K,N), suggesting that aberrant development is limited to BA1.

Forebrain defects in $Twsg1^{-/-}$ embryos are accompanied by loss of Shh and Fgf8 expression

The holoprosencephaly observed in $Twsg1^{-/-}$ mutants resembles that observed in $Chrd^{-/-};Nog^{+/-}$ mutants, which is caused by a loss of SHH signaling in the rostral mesendoderm (Anderson et al., 2002). Similarly, the ex-

pression of *Shh* in *Twsg1^{-/-}* embryos at E9.5 was significantly reduced in the ventral midline of the developing forebrain (Fig. 5B), suggesting a basis for the holoprosencephaly phenotype.

Although embryos lacking *Shh* have holoprosencephaly, they do not exhibit rostral truncations (Chiang et al., 1996), suggesting that additional molecular defects underlie the rostral truncations we observe. *Fgf8* expression in the ANR
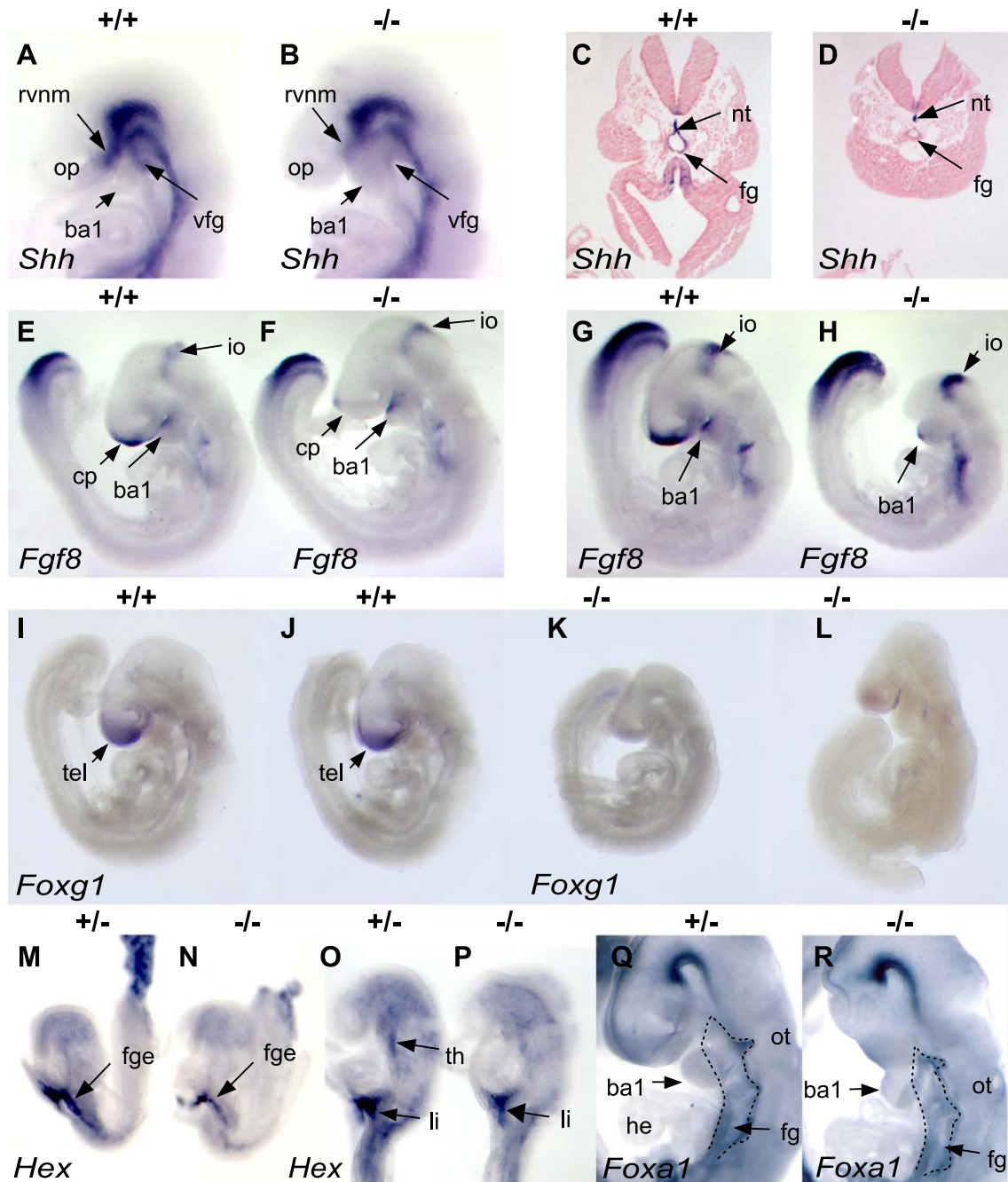

Fig. 5. Expression of *Shh* in E9.5 embryos. (A) Wild type; rostral ventral neural midline (rvnm); op, optic placode; ba1, first branchial arch; ventral foregut (vfg). (B) *Twsg1* mutant showing reduced expression in the rvnm. (C) Cross-section of the embryo shown in A. Notochord (nt) is closer to the foregut (fg). (D) Narrowing of the lumen of the foregut in the mutant shown in B. (E and G) *Fgf8* expression in a wild-type embryo at E9.5 in the commissural plate (cp), first branchial arch (ba1), and the isthmic organizer (io). (F) Reduced expression of *Fgf8* in the commissural plate of a mildly affected mutant, but normal expression in the first branchial arch and the isthmic organizer. (H) Absent rostral structures in severely affected mutant embryo; normal expression of *Fgf8* in the isthmic organizer (io). (I–J) Wild-type expression of *Foxg1* at E9.5 telencephalon (tel); (K–L) reduced *Foxg1* expression in E9.5 mutant. (M–P) Expression of *Hex* at four-somite-stage; (M) wild-type expression in the foregut endoderm (fge), (N) reduced expression in the mutants, (O and P) *Hex* expression at 10-somite-stage, (O) wild-type expression in the liver and thyroid domains, (P) absent expression of *Hex* in the mutants in the thyroid domain (th), and reduced expression in the liver domain (li). (Q) Wild-type *Foxa1* expression in the foregut, (R) reduction in the foregut extent of *Foxa1* expression in the mutants.

and derivative commissural plate plays an important role in the patterning of anterior neural structures, and its deletion in mice results in rostral truncations (Meyers et al., 1998). We found that approximately 25% of $Twsg1^{-/-}$ embryos (3 out of 12) showed variable degrees of reduction of $Fgf8$ expression specifically in the commissural plate (Figs. 5F,H), as in $Chrd^{-/-};Nog^{+/-}$ embryos, which display similar truncations (Anderson et al., 2002). All phenotypically abnormal $Twsg1^{-/-}$ embryos had reduced $Fgf8$ expression. In addition, the expression of a downstream target of FGF8, $Foxg1$ (previously known as $Bf1$), was reduced in the telencephalon (Figs. 5K,L), suggesting that FGF8 signaling may also be reduced (Shimamura and Rubenstein, 1997). In contrast, the expression of $Fgf8$ was normal in the isthmic organizer, even in the most severely affected embryos (Fig. 5H); this demonstrates that Twsg1 is not an obligate regulator of $Fgf8$ expression in brain development.

$Fgf8$ expression in proximal BA1 is necessary for mandibular outgrowth by promoting cell survival (Trumpp et al., 1999). Although the expression of $Fgf8$ is reduced in the first branchial arch in $Chrd^{-/-};Nog^{+/-}$ embryos and seems to account for the observed mandibular truncations (Stottmann et al., 2001), $Fgf8$ expression in BA1 of $Twsg1^{-/-}$ embryos is normal, suggesting a different mechanism for agnathia.

Deficient foregut endoderm development in Twsg1 homozygotes

In addition to craniofacial malformations, $Twsg1^{-/-}$ mice show abnormalities of the foregut. In $Twsg1$-deficient newborns, the oropharynx is rudimentary and maintains communication with the nasopharynx by forming a common cavity (Fig. 4P). To assess the origin of these defects, we examined foregut development during organogenesis. Histological sections of E9.5 mutant embryos revealed narrowing of the foregut lumen (Figs. 4H, L). In addition, we observed that the foregut was separated from the notochord in $Twsg1^{-/-}$ embryos, whereas in stage matched WT embryos, the notochord is contiguous with the foregut (Figs. 5C,D).

To further characterize defects in the foregut in $Twsg1^{-/-}$ mice, we examined the expression of foregut endodermal markers Hex (Bogue et al., 2000; Thomas et al., 1998) and $Foxa1$ (Ang et al., 1993). Hex-deficient mice have a reduced first branchial arch and forebrain truncations (Martinez Barbera et al., 2000). At the four-somite stage, expression of Hex was reduced in the foregut endoderm in $Twsg1^{-/-}$ mice (Fig. 5N). At the 10-somite stage, the expression of Hex was absent in the thyroid domain (Fig. 5P) and reduced in the liver domain (Fig. 5P). The expression of $Foxa1$ was unchanged in intensity, but the size of the foregut region was reduced in $Twsg1$ knockouts (Fig. 5R). Together, these data indicate that development of the foregut is impaired in the absence of $Twsg1$.

Discussion

Multiple roles for Twsg1 in modulating BMP signaling in mouse

In this paper we describe several phenotypes associated with loss of Twsg1 function during mouse development. The penetrance and spectrum of these phenotypes depend on the genetic background. In a hybrid 129Sv/Ev, C57BL/6, and FVB/N background, the most prevalent skeletal phenotype is truncation or loss of neural arches in the cervical and upper thoracic regions, while in a more inbred C57Bl/6 background numerous craniofacial malformations including severe rostral truncations, midline defects resulting in cyclopia or synophthalmia, and absence of the mandible are highly penetrant. We believe that these defects are likely the result of aberrant modulation of BMP signaling during embryogenesis. In the following discussion we will consider whether the phenotypes that we observe represent either pro- or anti-BMP effects. It is possible that the complex phenotypes that we observe might arise in part because in some regions and times Twsg1 has pro-BMP activity, while in other places and stages of development it has the opposite effect. It is also important to recognize that in some circumstances Twsg1 could have novel functions that are independent of BMP signaling. Twsg1 is a member of a broader family of secreted factors called the TIC superfamily that include both the insulin growth factor binding proteins (IGFBPs) and the CCN family of factors that include connective tissue growth factor (CTGF) (Vilmos et al., 2001). Many of these proteins can bind to distinct cell surface proteins of unknown identity, leaving open the possibility that they can elicit activation of distinct signal transduction cascades that are independent of BMPs or other known signaling molecules.

The neural arch defects in Twsg1$^{-/-}$ mice resemble the effects of ectopic BMP signaling

$Twsg1$-deficient mice had impaired formation of neural arches in the cervical and upper thoracic regions (spina bifida occulta) regardless of the genetic background. These defects resemble those observed in $Chrd$ homozygous null mice (Bachiller et al., 2003) as well as those produced by ectopic BMP signaling induced by grafting mouse BMP4- or human BMP2-producing cells in chick embryos (Monsoro-Burq et al., 1996), suggesting that the neural arch defects may result from excess BMP signaling. The molecular mechanism responsible for the loss of neural arch tissue remains elusive. Experiments in chick limb buds show that excessive BMP signaling that occurs before the formation of mesenchyme condensation results in the loss of a skeletal element through increased apoptosis (Duprez et al., 1996; Macias et al., 1997). We have been unable to detect a significant increase in apoptosis or decrease in proliferation of the condensing mesenchyme in the developing neural

arches of *Twsg1* mutant mice (unpublished data). An alternative explanation is that excess BMP signals at early stages in mesenchyme condensation might reduce the size of the founder cell population. Ultimately we should be able to address this issue when earlier markers of precondensing mesenchyme are identified.

While the defects that we observe within the neural arch are most consistent with Twsg1 and Chrd providing an antagonistic function towards BMP signaling in these regions other aspects of skeletal development may be affected differently. For example, in another recently targeted disruption of *Twsg1*, it has been reported that there is enlargement of the resting zones, but thinning of the proliferating and hypertrophic zones of distal growth plates in the femurs (Nosaka et al., 2003). Epiphyseal ossification has also been reported as reduced in these mice. The authors postulate that because delayed endochondral ossification resembles transgenic mice expressing a dominant-negative type IB BMP receptor, this particular skeletal phenotype might reflect attenuated BMP signaling and supports the role of Twsg1 as BMP agonist during skeletal growth of the long bones. We have not observed abnormalities within the growth plates of *Twsg1*$^{-/-}$ mice in a mixed genetic background. In our mice, the zones of resting, proliferating, and hypertrophic chondrocytes have normal width on longitudinal section of the knee joint (results not shown). Likewise, these authors did not report any defects within the cervical vertebrae. Given our observation that the phenotype exhibited by *Twsg1* mutant mice is strongly dependant on genetic background, it seems possible that these differences in skeletal phenotypes could reflect differences in the genetic makeup of the mice used in these two studies.

Anterior neural defects in Twsg1$^{-/-}$ *mice: pro- or anti-BMP effects?*

The holoprosencephaly and midline defects observed in *Twsg1*$^{-/-}$ mice strikingly resemble the phenotypes produced by simultaneous genetic ablation of the BMP antagonists Chrd and Nog in double mutants (*Chrd*$^{-/-}$;*Nog*$^{-/-}$ and *Chrd*$^{-/-}$; *Nog*$^{+/-}$) (Anderson et al., 2002; Bachiller et al., 2000). Similar phenotypes are also seen when the prechordal plate is surgically ablated in chick and mouse before the four-somite stage, suggesting that signals emanating from this tissue play a key role in patterning the forebrain (Pera and Kessel, 1997; Rubenstein and Beachy, 1998; Shimamura and Rubenstein, 1997). One such signal is *shh* which is expressed in the PrCP and mutations in either mouse or human *shh* result in severe midline defects (Chiang et al., 1996; Roessler and Muenke, 1998).

As found for *Chrd;Nog* double mutants, we observe a loss of *shh* expression in the rostral mesendoderm at day 9.5 suggesting that a reduction in *shh* is at least partially responsible for the *Twsg1*$^{-/-}$ holoprosencephaly phenotype. Because implantation of BMP-soaked beads in cephalic explants mimics the effects of loss of the BMP antagonists Chrd and Nog in double mutant embryos by downregulating expression of *shh* in the ventral midline (Anderson et al., 2002), the *Twsg1* loss-of-function phenotype also points to upregulation of BMP signaling as the basis for HPE. Likewise, ectopic application of recombinant BMP4 or BMP5 to the chicken forebrain leads to holoprosencephaly, cyclopia, and severely hypoplastic maxilla (Golden et al., 1999), a phenotype strikingly similar to that of *Twsg1*$^{-/-}$ mutants. Recent studies in Xenopus embryos also showed that loss of embryonic Tsg results in defects in both head and tail development as well as deficient eye development, all of which were attributable to excessive BMP signaling (Blitz et al., 2003).

However, there are several caveats that must be considered when interpreting these data. First, we have found that the penetrance of the severe craniofacial defects is very dependent on genetic background and is particularly enhanced in the C57BL/6J inbred strain. Previously, heterozygosity for Bmp4 on a C57Bl6/J background has also been shown to have enhanced craniofacial malformations, although these consisted primarily of reductions in the most rostral structures such as the frontal and nasal bones (Dunn et al., 1997). Nevertheless, this leaves open the possibility that a modifier present in C57BL6/J background independent of *Bmp4* is primarily responsible for the observed enhancement in the penetrance of the craniofacial defects. A second issue to consider is that in some tissues ectopic BMP4 can induce expression of its own antagonists (Stottman et al., 2001). Both Nog and Chrd were induced in mandibular explants by application of ectopic BMP4. Likewise, BMPs can also induce their own expression (Ghosh-Choudhury et al., 2001; Vainio et al., 1993) as well as the expression of inhibitory Smads (Afrakhte et al., 1998; Imamura et al., 1997). These complex regulatory relationships make it difficult to predict what the actual BMP activity levels are in different genetic backgrounds. The differences in genetic background as well as functional redundancy of BMP antagonists Chrd and Nog may also explain why we did not observe a genetic interaction between *Twsg1* and *Chrd* in causing HPE in double mutants in mixed genetic background. Mapping the *Twsg1* modifier in the C57BL/6 background together with an examination of the phenotypes produced by additional complex heterozygotes lacking other components of the BMP signaling pathway may help resolve these issues.

Although the midline defects in *Twsg1* null mutant embryos are most simply explained by the loss of *shh* expression, *shh* mutants do not exhibit mandible or rostral skeletal truncations as do *Twsg1*$^{-/-}$ mice (Chiang et al., 1996). This suggests that loss of *Twsg1* likely effects signals emanating from a second organizing center. One likely candidate is FGF8 produced in the anterior neural ridge. In some cases, loss of *Fgf8* from the ANR can recapitulate the rostral patterning defects seen in *Twsg1*$^{-/-}$ mice (Meyers et al., 1998). Our observation that *Fgf8* expression is specifically reduced in the ANR of *Twsg1*$^{-/-}$ mice

suggests that it may be a contributing factor to the truncation phenotype. Once again it is interesting to note that the $Chrd^{-/-};Nog^{+/-}$ mice exhibit the same spectrum of mandible and rostral truncation defects as found in $Twsg1^{-/-}$ mutants. In addition, they show a decrease of $Fgf8$ expression in the ANR (Anderson et al., 2002). Several BMPs are expressed in the anterior neuroectoderm and the adjacent nonneural ectoderm. Because ectopic BMP signaling from the ectoderm can repress $Fgf8$ in both chick and mouse ANR (Anderson et al., 2002; Ohkubo et al., 2002) as well as directly downregulate $Foxg1$ expression in the telencephalon (Furuta et al., 1997), it is possible that ectopic BMP signaling resulting from a loss of $Twsg1$ leads to the altered patterns of gene expression and the craniofacial phenotypes that we observe.

Expression of Twsg1 in the foregut endoderm is essential for normal patterning of the first branchial arch

In addition to the rostral and midline defects described above, $Twsg1$ mutant embryos also exhibit defects in the morphogenesis of the first branchial arch. The first branchial arch gives rise to the mandible, which is absent in 60% of affected $Twsg1^{-/-}$ embryos. All three germ layers and the neural crest contribute to the formation of the branchial arches. One signal that likely plays a role in BA1 patterning is $Fgf8$. Mouse embryos in which $Fgf8$ has been specifically removed from BA1 by Cre-mediated recombination or reduced by hypomorphic alleles of $Fgf8$ have jaw truncations similar to $Twsg1^{-/-}$ mice (Abu-Issa et al., 2002; Trumpp et al., 1999). In addition, $Chrd^{-/-}; Nog^{+/-}$ mice also show mandible truncations and a reduction in $Fgf8$ expression likely as a result of ectopic BMP expression (Stottmann et al., 2001). However, in $Twsg1^{-/-}$ mutant mice, we see no reduction in the expression of $Fgf8$ in BA1 and the morphology of the BA1 defect is different from that of $Chrd^{-/-}; Nog^{+/-}$ mutant mice. In $Twsg1$-deficient mice, the first branchial arch fails to subdivide into maxillary and mandibular components, and remains fused in the midline, whereas in $Chrd^{-/-}; Nog^{+/-}$ mutant mice BA1 exhibits varying degrees of hypoplasia likely caused by increased cell death (Stottmann et al., 2001). These observations suggest that the BA1 defects in $Twsg1$ mutant mice may have a different underlying cause than that which contributes to the phenotype in $Chrd^{-/-}; Nog^{+/-}$ mutants that is independent of BMP signaling. One possibility is that $Twsg1^{-/-}$ mice are defective in signals originating from the foregut. The foregut endoderm forms the inner layer of the pharyngeal pouches and provides instructive signals for their development (Piotrowski and Nusslein-Volhard, 2000; Trokovic et al., 2003). The ventral midline endoderm of the foregut has been proposed to act as a ventral head organizer in chick embryos (Kirby et al., 2003; Withington et al., 2001). We found that the foregut was underdeveloped in $Twsg1^{-/-}$ embryos and that expression of Hex, a homeobox containing the gene required in

definitive endoderm for normal forebrain and BA1 development, is reduced. The phenotype of moderate Hex mutants strikingly resembles that of $Twsg1$ mutant mice in that there are both forebrain defects and alterations in BA1 morphology including fusion at the midline (Martinez Barbera et al., 2000). The association between forebrain truncations and abnormalities of the first branchial arch suggests a common mechanism for these defects. Although forebrain defects in $Twsg1^{-/-}$ mice could be explained, at least in part, by reduced Shh expression in rostral ventral neural midline, alterations in foregut endoderm may be the primary defect that is influencing Shh expression. Hex expression was also affected in the thyroid domain of $Twsg1$ mutant mice. Even though we were able to identify thyroid glands in the mutants by gross examination, additional functional studies are needed to determine whether poor postnatal growth in $Twsg1^{-/-}$ mice could be caused by thyroid dysfunction.

Twsg1 is a candidate gene for holoprosencephaly

Holoprosencephaly is the most common structural anomaly of developing forebrain in humans with a prevalence of 1 in 10,000–20,000 live births and 1 in 250 during early embryogenesis (Muenke and Beachy, 2000). The etiology is heterogenous and includes both environmental and genetic factors. Chromosomal anomalies account for 20–40% of cases (Kinsman et al., 2000). Although mutations in several genes have been identified to date in patients in HPE, many candidate genes remain unknown. It is predicted that these genes are likely to map to at least 12 chromosomal regions on 11 chromosomes (Roessler and Muenke, 1998). The agnathia phenotype in $Twsg1$ mutant mice may provide a clue for narrowing the search for mutations in human HPE. $Twsg1$-null mice most closely resemble the human lethal malformation complex agnathia–holoprosencephaly, which is characterized by the absence of a mandible, positioning of ears toward the midline, and a series of defects of graded severity involving median malformations of the face and brain (Schiffer et al., 2002). A familial case of agnathia–holoprosencephaly has been reported to be associated with an inherited unbalanced translocation T(6,18)(p24.1;p11.21) (Pauli et al., 1983), which maps close to the $TWSG1$ chromosomal locus (18p11.3). It is therefore conceivable that $TWSG1$ mutations may be responsible for some cases of human HPE.

References

Abu-Issa, R., Smyth, G., Smoak, I., Yamamura, K., Meyers, E.N., 2002. Fgf8 is required for pharyngeal arch and cardiovascular development in the mouse. Development 129, 4613–4625.

Afrakhte, M., Moren, A., Jossan, S., Itoh, S., Sampath, K., Westermark, B., Heldin, C.H., Heldin, N.E., ten Dijke, P., 1998. Induction of inhibitory Smad6 and Smad7 mRNA by TGF-beta family members. Biochem. Biophys. Res. Commun. 249, 505–511.

Anderson, R.M., Lawrence, A.R., Stottmann, R.W., Bachiller, D., Klingensmith, J., 2002. Chordin and noggin promote organizing centers of forebrain development in the mouse. Development 129, 4975–4987.

Ang, S.L., Wierda, A., Wong, D., Stevens, K.A., Cascio, S., Rossant, J., Zaret, K.S., 1993. The formation and maintenance of the definitive endoderm lineage in the mouse: involvement of HNF3/forkhead proteins. Development 119, 1301–1315.

Bachiller, D., Klingensmith, J., Kemp, C., Belo, J.A., Anderson, R.M., May, S.R., McMahon, J.A., McMahon, A.P., Harland, R.M., Rossant, J., De Robertis, E.M., 2000. The organizer factors Chordin and Noggin are required for mouse forebrain development. Nature 403, 658–661.

Bachiller, D., Klingensmith, J., Shneyder, N., Tran, U., Anderson, R., Rossant, J., De Robertis, E.M., 2003. The role of chordin/Bmp signals in mammalian pharyngeal development and DiGeorge syndrome. Development 130, 3567–3578.

Blitz, I.L., Cho, K.W., Chang, C., 2003. Twisted gastrulation loss-of-function analyses support its role as a BMP inhibitor during early Xenopus embryogenesis. Development 130, 4975–4988.

Bogue, C.W., Ganea, G.R., Sturm, E., Ianucci, R., Jacobs, H.C., 2000. Hex expression suggests a role in the development and function of organs derived from foregut endoderm. Dev. Dyn. 219, 84–89.

Chang, C., Holtzman, D.A., Chau, S., Chickering, T., Woolf, E.A., Holmgren, L.M., Bodorova, J., Gearing, D.P., Holmes, W.E., Brivanlou, A.H., 2001. Twisted gastrulation can function as a BMP antagonist. Nature 410, 483–487.

Chiang, C., Litingtung, Y., Lee, E., Young, K.E., Corden, J.L., Westphal, H., Beachy, P.A., 1996. Cyclopia and defective axial patterning in mice lacking Sonic hedgehog gene function. Nature 383, 407–413.

Couly, G., Creuzet, S., Bennaceur, S., Vincent, C., Le Douarin, N.M., 2002. Interactions between Hox-negative cephalic neural crest cells and the foregut endoderm in patterning the facial skeleton in the vertebrate head. Development 129, 1061–1073.

Crossley, P.H., Martin, G.R., 1995. The mouse Fgf8 gene encodes a family of polypeptides and is expressed in regions that direct outgrowth and patterning in the developing embryo. Development 121, 439–451.

Dunn, N.R., Winnier, G.E., Hargett, L.K., Schrick, J.J., Fogo, A.B., Hogan, B.L., 1997. Haploinsufficient phenotypes in Bmp4 heterozygous null mice and modification by mutations in Gli3 and Alx4. Dev. Biol. 188, 235–247.

Duprez, D., Bell, E.J., Richardson, M.K., Archer, C.W., Wolpert, L., Brickell, P.M., Francis-West, P.H., 1996. Overexpression of BMP-2 and BMP-4 alters the size and shape of developing skeletal elements in the chick limb. Mech. Dev. 57, 145–157.

Echelard, Y., Epstein, D.J., St.-Jacques, B., Shen, L., Mohler, J., McMahon, J.A., McMahon, A.P., 1993. Sonic hedgehog, a member of a family of putative signaling molecules, is implicated in the regulation of CNS polarity. Cell 75, 1417–1430.

Furuta, Y., Piston, D.W., Hogan, B.L., 1997. Bone morphogenetic proteins (BMPs) as regulators of dorsal forebrain development. Development 124, 2203–2212.

Ghosh-Choudhury, N., Choudhury, G.G., Harris, M.A., Wozney, J., Mundy, G.R., Abboud, S.L., Harris, S.E., 2001. Autoregulation of mouse BMP-2 gene transcription is directed by the proximal promoter element. Biochem. Biophys. Res. Commun. 286, 101–108.

Golden, J.A., Bracilovic, A., McFadden, K.A., Beesley, J.S., Rubenstein, J.L., Grinspan, J.B., 1999. Ectopic bone morphogenetic proteins 5 and 4 in the chicken forebrain lead to cyclopia and holoprosencephaly. Proc. Natl. Acad. Sci. U. S. A. 96, 2439–2444.

Graf, D., Timmons, P.M., Hitchins, M., Episkopou, V., Moore, G., Ito, T., Fujiyama, A., Fisher, A.G., Merkenschlager, M., 2001. Evolutionary conservation, developmental expression, and genomic mapping of mammalian twisted gastrulation. Mamm. Genome 12, 554–560.

Hogan, B.L., 1996. Bone morphogenetic proteins: multifunctional regulators of vertebrate development. Genes Dev. 10, 1580–1594.

Hogan, B., Beddington, R., Constantini, F., Lacy, E., 1994. Manipulating the Mouse Embryo. A Laboratory Manual. Cold Spring Harbor Laboratory Press, New York.

Imamura, T., Takase, M., Nishihara, A., Oeda, E., Hanai, J., Kawabata, M., Miyazono, K., 1997. Smad6 inhibits signalling by the TGF-beta superfamily. Nature 389, 622–626.

Kinsman, S.L., Plawner, L.L., Hahn, J.S., 2000. Holoprosencephaly: recent advances and new insights. Curr. Opin. Neurol. 13, 127–132.

Kirby, M.L., Lawson, A., Stadt, H.A., Kumiski, D.H., Wallis, K.T., McCraney, E., Waldo, K.L., Li, Y.X., Schoenwolf, G.C., 2003. Hensen's node gives rise to the ventral midline of the foregut: implications for organizing head and heart development. Dev. Biol. 253, 175–188.

Larrain, J., Oelgeschlager, M., Ketpura, N.I., Reversade, B., Zakin, L., De Robertis, E.M., 2001. Proteolytic cleavage of Chordin as a switch for the dual activities of twisted gastrulation in BMP signaling. Development 128, 4439–4447.

Lawson, K.A., Dunn, N.R., Roelen, B.A., Zeinstra, L.M., Davis, A.M., Wright, C.V., Korving, J.P., Hogan, B.L., 1999. Bmp4 is required for the generation of primordial germ cells in the mouse embryo. Genes Dev. 13, 424–436.

Lewandoski, M., Meyers, E.N., Martin, G.R., 1997. Analysis of Fgf8 gene function in vertebrate development. Cold Spring Harbor Symp. Quant. Biol. 62, 159–168.

Macias, D., Ganan, Y., Sampath, T.K., Piedra, M.E., Ros, M.A., Hurle, J.M., 1997. Role of BMP-2 and OP-1 (BMP-7) in programmed cell death and skeletogenesis during chick limb development. Development 124, 1109–1117.

Martinez Barbera, J.P., Clements, M., Thomas, P., Rodriguez, T., Meloy, D., Kioussis, D., Beddington, R.S., 2000. The homeobox gene Hex is required in definitive endodermal tissues for normal forebrain, liver and thyroid formation. Development 127, 2433–2445.

Meyers, E.N., Lewandoski, M., Martin, G.R., 1998. An Fgf8 mutant allelic series generated by Cre- and Flp-mediated recombination. Nat. Genet. 18, 136–141.

Monsoro-Burq, A.H., Duprez, D., Watanabe, Y., Bontoux, M., Vincent, C., Brickell, P., Le Douarin, N., 1996. The role of bone morphogenetic proteins in vertebral development. Development 122, 3607–3616.

Muenke, M., Beachy, P.A., 2000. Genetics of ventral forebrain development and holoprosencephaly. Curr. Opin. Genet. Dev. 10, 262–269.

Nosaka, T., Morita, S., Kitamura, H., Nakajima, H., Shibata, F., Morikawa, Y., Kataoka, Y., Ebihara, Y., Kawashima, T., Itoh, T., Ozaki, K., Senba, E., Tsuji, K., Makishima, F., Yoshida, N., Kitamura, T., 2003. Mammalian twisted gastrulation is essential for skeleto-lymphogenesis. Mol. Cell. Biol. 23, 2969–2980.

Oelgeschlager, M., Larrain, J., Geissert, D., De Robertis, E.M., 2000. The evolutionarily conserved BMP-binding protein Twisted gastrulation promotes BMP signalling. Nature 405, 757–763.

Oelgeschlager, M., Reversade, B., Larrain, J., Little, S., Mullins, M.C., De Robertis, E.M., 2003. The pro-BMP activity of Twisted gastrulation is independent of BMP binding. Development 130, 4047–4056.

Ohkubo, Y., Chiang, C., Rubenstein, J.L., 2002. Coordinate regulation and synergistic actions of BMP4, SHH and FGF8 in the rostral prosence-

phalon regulate morphogenesis of the telencephalic and optic vesicles. Neuroscience 111, 1–17.

Pauli, R.M., Pettersen, J.C., Arya, S., Gilbert, E.F., 1983. Familial agnathia–holoprosencephaly. Am. J. Med. Genet. 14, 677–698.

Pera, E.M., Kessel, M., 1997. Patterning of the chick forebrain anlage by the prechordal plate. Development 124, 4153–4162.

Petryk, A., Fleenor, D., Driscoll, P., Freemark, M., 2000. Prolactin induction of insulin gene expression: the roles of glucose and glucose transporter-2. J. Endocrinol. 164, 277–286.

Piotrowski, T., Nusslein-Volhard, C., 2000. The endoderm plays an important role in patterning the segmented pharyngeal region in zebrafish (*Danio rerio*). Dev. Biol. 225, 339–356.

Raymond, C.S., Murphy, M.W., O'Sullivan, M.G., Bardwell, V.J., Zarkower, D., 2000. Dmrt1, a gene related to worm and fly sexual regulators, is required for mammalian testis differentiation. Genes Dev. 14, 2587–2595.

Rodriguez, C.I., Buchholz, F., Galloway, J., Sequerra, R., Kasper, J., Ayala, R., Stewart, A.F., Dymecki, S.M., 2000. High-efficiency deleter mice show that FLPe is an alternative to Cre-loxP. Nat. Genet. 25, 139–140.

Roessler, E., Muenke, M., 1998. Holoprosencephaly: a paradigm for the complex genetics of brain development. J. Inherited Metab. Dis. 21, 481–497.

Ross, J.J., Shimmi, O., Vilmos, P., Petryk, A., Kim, H., Gaudenz, K., Hermanson, S., Ekker, S.C., O'Connor, M.B., Marsh, J.L., 2001. Twisted gastrulation is a conserved extracellular BMP antagonist. Nature 410, 479–483.

Rubenstein, J.L., Beachy, P.A., 1998. Patterning of the embryonic forebrain. Curr. Opin. Neurobiol. 8, 18–26.

Sasaki, H., Hogan, B.L., 1993. Differential expression of multiple fork head related genes during gastrulation and axial pattern formation in the mouse embryo. Development 118, 47–59.

Schiffer, C., Tariverdian, G., Schiesser, M., Thomas, M.C., Sergi, C., 2002. Agnathia–otocephaly complex: report of three cases with involvement of two different Carnegie stages. Am. J. Med. Genet. 112, 203–208.

Schneider, R.A., Hu, D., Rubenstein, J.L., Maden, M., Helms, J.A., 2001. Local retinoid signaling coordinates forebrain and facial morphogenesis by maintaining FGF8 and SHH. Development 128, 2755–2767.

Scott, I.C., Blitz, I.L., Pappano, W.N., Maas, S.A., Cho, K.W., Greenspan, D.S., 2001. Homologues of Twisted gastrulation are extracellular cofactors in antagonism of BMP signalling. Nature 410, 475–478.

Shimamura, K., Rubenstein, J.L., 1997. Inductive interactions direct early regionalization of the mouse forebrain. Development 124, 2709–2718.

Storm, E.E., Rubenstein, J.L., Martin, G.R., 2003. Dosage of Fgf8 determines whether cell survival is positively or negatively regulated in the developing forebrain. Proc. Natl. Acad. Sci. U. S. A. 100, 1757–1762.

Stottmann, R.W., Anderson, R.M., Klingensmith, J., 2001. The BMP antagonists Chordin and Noggin have essential but redundant roles in mouse mandibular outgrowth. Dev. Biol. 240, 457–473.

Tao, W., Lai, E., 1992. Telencephalon-restricted expression of BF-1, a new member of the HNF-3/fork head gene family, in the developing rat brain. Neuron 8, 957–966.

Thomas, P.Q., Brown, A., Beddington, R.S., 1998. Hex: a homeobox gene revealing peri-implantation asymmetry in the mouse embryo and an early transient marker of endothelial cell precursors. Development 125, 85–94.

Trokovic, N., Trokovic, R., Mai, P., Partanen, J., 2003. Fgfr1 regulates patterning of the pharyngeal region. Genes Dev. 17, 141–153.

Trumpp, A., Depew, M.J., Rubenstein, J.L., Bishop, J.M., Martin, G.R., 1999. Cre-mediated gene inactivation demonstrates that FGF8 is required for cell survival and patterning of the first branchial arch. Genes Dev. 13, 3136–3148.

Vainio, S., Karavanova, I., Jowett, A., Thesleff, I., 1993. Identification of BMP-4 as a signal mediating secondary induction between epithelial and mesenchymal tissues during early tooth development. Cell 75, 45–58.

Vilmos, P., Gaudenz, K., Hegedus, Z., Marsh, J.L., 2001. The Twisted gastrulation family of proteins, together with the IGFBP and CCN families, comprise the TIC superfamily of cysteine rich secreted factors. J. Clin. Pathol.: Mol. Pathol. 54, 317–323.

Wilkinson, D.G., Nieto, M.A., 1993. Detection of messenger RNA by in situ hybridization to tissue sections and whole mounts. Methods Enzymol. 225, 361–373.

Withington, S., Beddington, R., Cooke, J., 2001. Foregut endoderm is required at head process stages for anteriormost neural patterning in chick. Development 128, 309–320.